

Compositional Mapping by Laser-Induced Breakdown Spectroscopy

Taesam Kim and C. T. Lin*

Department of Chemistry and Biochemistry, Northern Illinois University, DeKalb, Illinois 60115-2862

Yoonyeol Yoon

Korea Institute of Geology and Material, 30 Kajungdong, Yousung, Taejon, Korea

Received: November 18, 1997; In Final Form: February 27, 1998

A sensitive optical technique for compositional mapping of solid surfaces using laser-induced breakdown spectroscopy (LIBS) is described. A pulsed Nd:YAG laser with second harmonic module was focused on the solid surface, giving a small ablation area, to produce plasma emission. Copper and magnesium emissions from a standard sample were carefully analyzed and assigned in the wavelength range 500–520 nm. The assigned spectral information was selected to construct an image of 100×100 pixels by mapping the measured emission intensity values from the analyzed points. The time required for image construction and image sharpness depends on the number of laser shots per point of analysis and the number of analyzed points per image. A clear image of a copper conductor pattern from a printed circuit board was generated. In addition, some copper contaminations around the conductor area are clearly visible in the scanning LIBS map. The contaminated copper salt probably resulted from the incomplete washing step during manufacturing that could cause a short circuit in an electronic device.

Introduction

The compositional map of a solid surface layer can offer important information about the quantitative chemical distribution of the materials that is essential to the industrial manufacturer and quality control scientist. One of the available surface analytical techniques that can give the spatial distribution of elements in a sample is the energy-dispersive X-ray (EDX) method. The EDX equipment is generally combined with a scanning electron microscope (SEM), providing a convenient way to record the real and compositional images on an enlarged microsize sample.¹ However, the measurable sensitivity of the EDX technique is limited² only to about a few percent, and it becomes worse for the light elements because of their weak X-ray emission. Moreover, the EDX spectra can overlap between elements with K, L, and M shells of X-ray origins that tend to mislead the proper determination of chemical compositions.³ Other surface techniques are Auger electron spectroscopy (AES) and Rutherford backscattering (BRS) which use an electron and ion beam, respectively. Both AES and BRS require a vacuum system and may cause charging problems on a dielectric sample.

Focused light from a high-power laser can induce breakdown discharges and generate plasmas, and it has been used as an excitation source for inducing atomic emission in chemical analysis. Over the past few years, a considerable number of studies have been conducted on laser-induced breakdown spectroscopy (LIBS).⁴ The strong impact of intense laser light on solid materials causes sample ablation, vaporization, and ionization. The high temperature and high electron density plasma formed results in ions, electrons, and electronically excited atoms and clusters. The plasma emission can be analyzed spatially and temporally to determine the chemical

species and their concentrations.⁵ LIBS has been applied to bulk materials, to depth profile characterization,⁶ and on site analysis⁷ for different forms of samples, including gas,⁸ solution,⁹ soil,¹⁰ and metal.¹¹ LIBS has also been used to generate volatile chemical species in conjunction with other analytical techniques such as mass spectrometry.

In a specific application, LIBS was employed to determine the elemental composition of contaminants found on electronic microcircuits fabricated on alumina substrates.¹² In this paper, LIBS is used to detect laser spark emission in a small surface area for compositional mapping of solid materials. The plasma emission monitored for a specific chemical element obtained from scanning LIBS gives compositional distribution and thus an image of the surface display. The spatial resolution limit of an image caused by the laser ablating conditions is examined. The possible extension of LIBS to samples with multiple elements, elements with different lifetimes, and materials with different depth profile characteristics is also discussed.

Experimental Section

The experimental setup for laser-induced breakdown spectroscopy is shown schematically in Figure 1. A pulsed Nd:YAG laser with a second harmonic module (Spectron, model SL802, wavelength 532 nm and pulse width 10 ns) was operated at a repetition rate of 5 Hz and used to produce plasma emission at room temperature in air. Laser light is focused onto solid samples with a convex lens ($f = 34$ mm). The laser energy is 5 mJ if not otherwise mentioned. The solid sample is placed on a support which is fixed on a bidimensional translation XY stage. The mechanical stage is tilted 30° from the horizontal to maintain an identical optical pathway for each laser ablating point during the stage movement. The sample supporting stage moves along the X and Y axes by two stepping motors combined with micrometers. Each moving step size is adjusted to be 50

* To whom correspondence should be addressed.

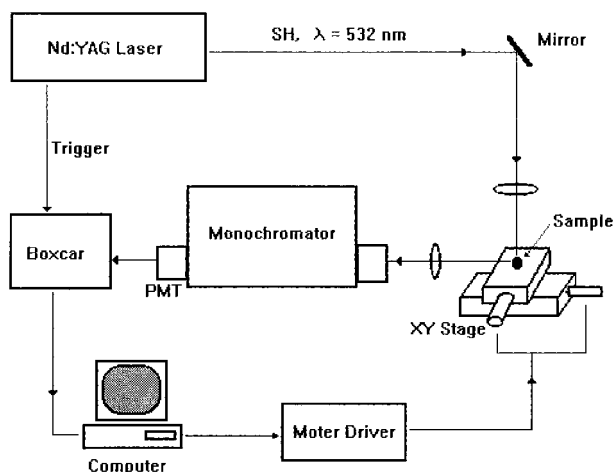


Figure 1. A schematic diagram of an experimental setup used for compositional mapping of a solid sample.

μm to prevent any overlapping from the previously ablated spot. The plasma emission is focused by a pair of optical lenses and detected with a PMT (Hamamatsu, R928) via a double-grating spectrometer (SPEX, model 1403, $F/\# = 7.8$). The plasma plume axis is parallel to the entrance slit of a spectrometer which has a spectral resolution of 0.5 nm. The emission signal from a PMT is captured with a boxcar integrator (SRS 250) synchronized by a delay pulse generator (DG 535), operating at a delay time of 3 μs . A PC is used to program the boxcar integrator for acquiring emission data at the predetermined number of laser pulses and also for controlling the stage translation mechanism to move the sample from one to the next laser ablating area.

A standard aluminum alloy (SPEX, #888-5), containing 91.4% Al, 5.1% Cu, 1.0% Mg, 0.77% Mn, 0.55% Fe, 0.49% Ni, 0.46% Si, 0.2% Zn, and others, was used to select and characterize the emission peak of the desired elements. A printed circuit board available commercially from an electronics industry was employed for the compositional mapping of Cu using LIBS.

Results and Discussion

Characterization and Selection of Plasma Emission Lines for the Desired Elements. The laser spark emission of a metallic element is generally displayed in a well-defined spectral region. However, there are also spectral ranges where the plasma emission lines are densely overlapped by spectral lines of other metal components. Therefore, the spectroscopic characterization of LIBS on a standard metal alloy is a necessary initial step to carefully identify a spectral line for compositional mapping of the desired metal element. For single-element compositional mapping by LIBS, an intense and well-isolated plasma emission line is generally preferred.

The laser-induced plasma of the SPEX #888-5 alloy showed strong emission corresponding to aluminum at $\lambda < 400$ nm, copper at $\lambda \sim 500\text{--}516$ nm, and magnesium at $\lambda \sim 516\text{--}520$ nm. For the purpose of this study, Figure 2 shows only a small spectral region of plasma emission of standard aluminum alloy induced by LIBS, i.e., the copper and magnesium emission in the wavelength range 510–520 nm. The emission spectrum displayed in Figure 2 is a time-integrated intensity of five laser shots at each wavelength, and the scanning monochromator moves at a wavelength step of 0.5 nm. The spectral peak assignments in Figure 2 are made by using reference values¹³

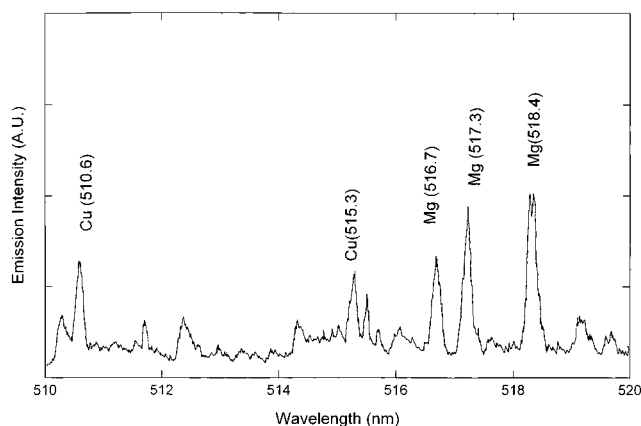


Figure 2. Spark emission of copper and manganese obtained from LIBS of aluminum alloy (SPEX #888-5).

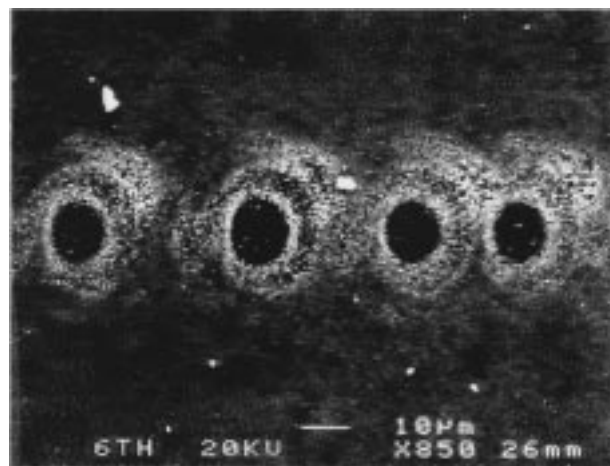


Figure 3. SEM image of ablated spot and crater formed on the copper surface by LIBS.

and the known composition of the standard metal alloy (i.e., SPEX #888-5). It is also important to note that the absolute intensity of plasma emission in LIBS depends on the laser power applied. The higher laser power induces stronger plasma emission, but the use of a high-power laser tends to generate a high background of white light emission. The experimentally determined laser energy for an optimum copper plasma emission and minimum white light is 5 mJ. The reduction of background white light can also be accomplished by using a UV laser as an excitation source¹⁴ or by detecting plasma emission in the UV spectral range.

For many practical applications of LIBS in spectroscopy and also in compositional mapping, great care must be exercised to control the spark plasma emission of the metal element present in the analytical sample. For example, the emission intensity and spectral distribution of the plasma produced by LIBS are very sensitive to gas pressure and gas flow surrounding the plasma plume. A large enhancement of the S/N ratio in spark plasma emission has been reported^{14,15} in an inert gas atmosphere. In this study, we were able to achieve a reproducibility of $\sigma = 5\%$ in plasma emission intensity (shot-by-shot fluctuation) under a nitrogen atmosphere. Under our experimental conditions, the useful plasma emission for copper ranges from 510.6 to 515.3 nm and is displayed in Figure 2. The intense and well-separated emission line at $\lambda = 510.6$ nm was selected for compositional mapping of copper on a printed circuit board.

Microscopic View of Laser Ablating Area. The laser-ablated area for each measured pixel is controlled by the focused laser beam size. Figure 3 displays an electron microscopic view

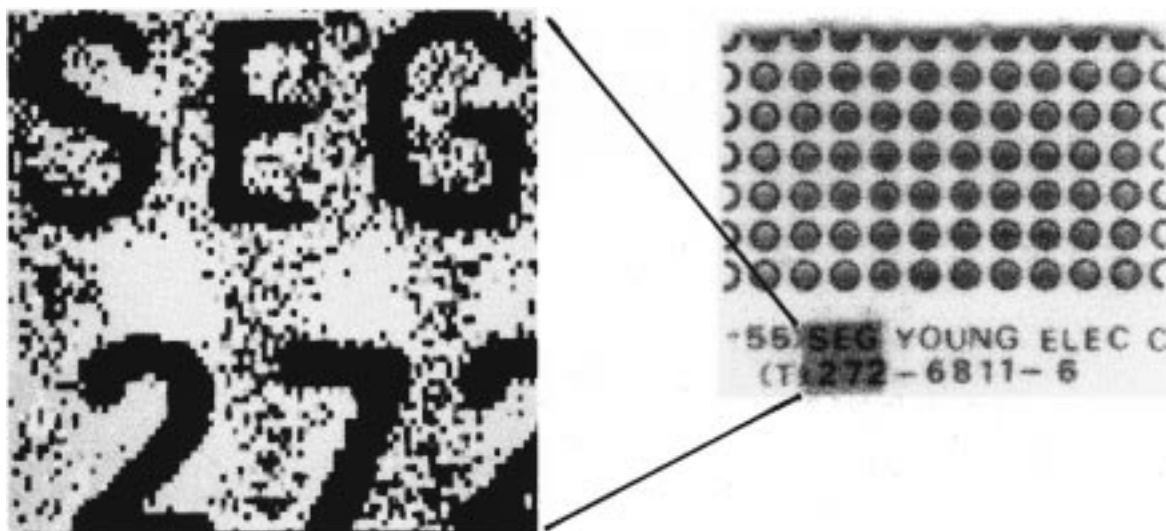


Figure 4. (right) A commercial printed circuit board. Circles on top are patterned copper layer for soldering the electronic components. Characters on the bottom are the same copper layer for product identification. The laser-ablated area (gray shaded square) is $5 \times 5 \text{ mm}^2$. (left) A mapping image of copper corresponding to the gray shaded square. Each 100×100 pixels corresponds to a measured emission intensity value of LIBS on the ablated point.

of a laser-ablated surface of a printed circuit board made by our experimental setup with optimum conditions. The formation of a crater around each laser ablated area is clearly observed. The diameter of the ablated area is about $10 \mu\text{m}$ whereas the thermally damaged crater size is about $25 \mu\text{m}$. Since the distance between one and the next ablated area is $50 \mu\text{m}$, no overlap of ablated material from one site to the next is observed in Figure 3. The optimum experimental conditions obtained in Figure 3 are employed for the compositional mapping of copper in the commercial printed circuit board.

Elemental Mapping of Copper Using LIBS. The image on the left-hand side of Figure 4 displays a LIBS mapping of copper plasma emission from a selected $5 \times 5 \text{ mm}^2$ area (right-hand side of Figure 4) of a printed circuit board. One image of 100×100 pixels can be obtained in about 30–120 min depending on the number of laser pulses used for data averaging (i.e., the number of laser shots per point of analysis and the number of analyzed points per image). Experimentally, the total emission from the copper plasma at $\lambda = 510.6 \text{ nm}$ was accumulated regardless of the area size of the plasma plume or the time-delayed factor between the laser fire and the emission signal captured by the boxcar integrator. The base material of the circuit board is composed of a mixture of glass fiber and epoxy resin. The compositional image of Figure 4 gives a clear pattern of the elemental copper which resembles the standard 0.2 mm thickness of the copper layer fabricated in a printed circuit board. A careful examination of Figure 4 reveals that some contaminated copper stains are visible between the copper conductor area. A thick copper stain, if connected between the conductor patterns, may cause an electronic short circuit. It is noted that the collective copper stain displays a streamline shape flowing from the conducting copper islands. Thus, the stained copper contamination presumably resulted from the fabrication processing of the printed circuit board. The standard procedure for patterning the circuit board starts with a lithographic development, etching with ferric chloride solution, and followed by rinsing and drying. The direction of the copper stain displayed in Figure 4 shows that the circuit board was dried upright without a complete rinsing of the etching solution during the manufacturing process. The stained copper contamination

can be seen more clearly with color rendering (not shown), corresponding to the emission intensity value of each ablating point.

A larger laser energy of 10 mJ tended to produce a blurred compositional image. At a laser energy of 10 mJ or more, the ejected particles from one ablated crater are scattered around the ablating area contaminating the next ablated site. This contamination around the ablated crater can be reduced by rapidly flowing nitrogen gas stream to blow off the ejected particles from the laser ablating surface. The in situ surface cleaning with a nitrogen gas stream is effective when the flow rate of nitrogen gas is greater than 10 mL/min through a 1 mm diameter nozzle. No effect is observed under a static nitrogen atmosphere.

The technique of compositional mapping by LIBS can offer several distinct advantages in the determination of elemental distributions on a solid surface involving multiple elements. In principle, the elemental concentration in a solid sample can be measured directly via a well-calibrated intensity of plasma spark emission. The technique is very sensitive to many metallic elements, especially those that have been characterized by atomic emission spectroscopy (such as ICP-AES and ARC-AES). The LIBS technique can be applied on a realistic commercial sample with large physical dimensions. In practice, the scanning LIBS mapping is suitable for a few millimeters size of sample, which is not the convenient sample size for the SEM/EDX technique. The common EDX measurement is oriented to micrometer scale mapping. It is difficult to design a compositional mapping technique, except for the scanning LIBS mapping method described in this paper, that is convenient for measuring a millimeter or larger size of solid surface.

The present scanning LIBS mapping method can be easily extended to a simultaneous measurement of several elements by using an optical multichannel analyzer. Since each element in a multielement sample has a distinctive spark emission lifetime, it is possible to gate the optical multichannel analyzer at a specific time delay which can then be used to obtain a temporal distribution of compositional mapping. The delay time should be carefully selected to obtain better results depending on the prospective elements in the solid sample. The LIBS technique for time-resolved and selective elemental distribution

of compositional mapping by LIBS is currently under development in our laboratory.

Conclusion

A clear image of a printed circuit board has been obtained for the compositional mapping of a copper conductor by laser-induced breakdown spectroscopy. The scanning LIBS mapping of a 100×100 pixels size can be accomplished in about $1/2$ –2 h. The surface contamination of a copper stain in the commercial printed circuit board has been clearly characterized. The technique of LIBS is shown to display high sensitivity, selectivity, wide dynamic range, and versatility over other analytical techniques. In particular, the scanning LIBS is an ideal technique for in situ analysis of surface contamination and depth profiling of industrial samples.

Acknowledgment. T.K. would like to thank Korea Science and Engineering Foundation for a fellowship award.

References and Notes

- (1) Pirs, J.; Zalar, A. *Michimica Acta* **1990**, *II*, 295.
- (2) Orts, M. J.; Rincon, J. M.; Rivera, E.; Celaya, L. E. *Mater. Lett.* **1988**, *7* (3), 106.
- (3) Houk, C. S.; Page, C. J. *Adv. Mater.* **1996**, *8* (2), 173.
- (4) Russo, R. E. *Appl. Spectrosc.* **1995**, *49* (9), 14A.
- (5) Castle, B. C.; Visser, K.; Smith, B. W.; Winefordner, J. D. *Appl. Spectrosc.* **1997**, *51* (7), 1017.
- (6) Anglos, D.; Couris, S.; Fotakis, C. *Appl. Spectrosc.* **1997**, *51* (7), 1025.
- (7) Marquardt, B. J.; Goode, S. R.; Anger, S. M. *Anal. Chem.* **1996**, *68*, 977.
- (8) Nordstrom, R. J. *Appl. Spectrosc.* **1995**, *49* (10), 1490.
- (9) Ito, Y.; Ueki, O.; Nakamura, S. *Anal. Chem. Acta* **1995**, *299*, 401.
- (10) Eppler, A. S.; Cremers, D. A.; Hickmott, D. D.; Ferris, M. J.; Koskelo, A. C. *Appl. Spectrosc.* **1996**, *50* (9), 1175.
- (11) Satlman, R.; Strum, V.; Noll, R. *J. Phys. D: Appl. Phys.* **1995**, *28*, 2181.
- (12) Ottesen, D. K. *Appl. Spectrosc.* **1992**, *46* (4), 593.
- (13) Fernandez, A.; Mao, X. L.; Chan, W. T.; Shannon, M. A.; Russo, R. E. *Anal. Chem.* **1995**, *67* (14), 2444.
- (14) Lee, Y. I.; Song, K.; Cha, H.; Lee, J.; Park, M.; Lee, G.; Sneddon, J. *Appl. Spectrosc.* **1997**, *51* (7), 959.
- (15) Thiem, T. L.; Salter, R. H.; Gardner, J. A.; Lee, Y. I.; Sneddon, J. *Appl. Spectrosc.* **1994**, *48* (1), 58.